HHS Public Access

Author manuscript

Nat Struct Mol Biol. Author manuscript; available in PMC 2010 February 01.

Published in final edited form as:

Nat Struct Mol Biol. 2009 August ; 16(8): 814–818. doi:10.1038/nsmb.1640.

Role of mammalian Mre11 in classical and alternative non-homologous end joining

Anyong Xie[1], **Amy Kwok**, and **Ralph Scully**[1]

Department of Medicine, Harvard Medical School and Beth Israel Deaconess Medical Center, 330 Brookline Avenue, Boston, MA 02215

Abstract

The mammalian Mre11-Rad50-Nbs1 (MRN) complex coordinates double strand break (DSB) signaling with repair by homologous recombination and is associated with the H2A.X chromatin response to DSBs, but its role in non-homologous end joining (NHEJ) is less clear. Here we show that Mre11 promotes efficient NHEJ in both wild-type and *Xrcc4*$^{-/-}$ mouse embryonic stem cells. Depletion of Mre11 reduces use of microhomology during NHEJ in *Xrcc4*$^{+/+}$ cells and suppresses end resection in *Xrcc4*$^{-/-}$ cells, revealing specific roles for Mre11 in both classical and alternative NHEJ. The NHEJ function of Mre11 is independent of *H2A.X*. We propose a model in which both enzymatic and scaffolding functions of Mre11 cooperate to support mammalian NHEJ.

DNA double strand breaks (DSBs) provoke a complex set of cellular responses, which, if defective, can perturb development or promote cancer in higher eukaryotes. The Mre11/Rad50/Nbs1 (MRN) complex in vertebrates and the homologous Mre11/Rad50/Xrs2 (MRX) complex in yeast act as DSB sensors and also support DSB repair 1. MRN binds to DNA ends, recruiting and activating the Atm signaling kinase 2,3. One of the targets of Atm is histone H2A.X, which is phosphorylated on serine 139 to form "γ-H2A.X", recruiting Mdc1, MRN and other protein complexes to chromatin near the DSB 4. Thus, MRN exists in two fractions near the DSB – an *H2A.X*-independent fraction at the DSB and an *H2A.X/Mdc1*-dependent fraction on chromatin 5. Loss of *Mre11*, *Rad50* or *Nbs1* results in embryonic lethality in mice 6-8. Hypomorphic mutations in human *MRE11* or *NBS1* lead to ataxia telangiectasia-like disorder (ATLD) or Nijmegen breakage syndrome (NBS) respectively 9,10. Cells derived from individuals with either disorder show radiation hypersensitivity, chromosomal instability and DSB repair defects.

DSBs in eukaryotes are repaired primarily by homologous recombination (HR) or non-homologous end joining (NHEJ). In mammalian cells, the classical NHEJ pathway uses Xrcc4/DNA ligase 4 to catalyze ligation of DNA ends 11,12. A robust alternative, *Xrcc4*-independent NHEJ pathway has been identified 13-16. DSB repair products in *Xrcc4*$^{-/-}$

[1] Corresponding authors: R.S. rscully@bidmc.harvard.edu. Telephone 617-735-2045. Fax 617-735-2222; A.X. axie@bidmc.harvard.edu Telephone 617-735-2042. Fax 617-735-2222.

AUTHOR CONTRIBUTIONS

A.X. designed and performed the experiments. R.S. participated in the design of the experiments. A.K. assisted on Southern blotting and DNA sequencing. A.X. and R.S. analyzed the data and wrote the manuscript.

cells reveal frequent deletions associated with short tracts of homology at the repair junction, an outcome termed microhomology-mediated end joining (MMEJ) 17.

The MRN complex has been implicated in HR in both yeast and vertebrates. Mre11 collaborates with Sae2/Ctp1/CtIP in end processing for HR 18-21, and MRN/MRX may also promote HR by tethering DNA ends 22-24. In *Saccharomyces cerevisiae*, MRX facilitates NHEJ 25,26 and has also been implicated in MMEJ 27. Early efforts to demonstrate a role for vertebrate MRN in NHEJ led to contradictory conclusions 28-30. However, recent work has revealed a role for MRN in NHEJ during V(D)J recombination in developing immunocytes 31,32. To what extent mammalian MRN influences NHEJ of unscheduled DSBs is not clear.

To study the role of Mre11 in mammalian NHEJ, including *Xrcc4*-independent NHEJ, we generated isogenic *Xrcc4*$^{+/+}$ and *Xrcc4*$^{-/-}$ mouse embryonic stem (ES) cells harboring a single copy of an NHEJ reporter, in which NHEJ is triggered in response to tandem site-specific chromosomal DSBs. Our work reveals a critical role for Mre11 in both *Xrcc4*-dependent and *Xrcc4*-independent NHEJ in mammalian cells and suggests that Mre11 participates in the processing of DSBs for MMEJ in cells lacking *Xrcc4*.

RESULTS

We developed NHEJ reporters in which translation of a wild-type copy of the gene encoding enhanced green fluorescent protein ("*GFP*") is suppressed by an upstream, out-of-frame translation start site ("*Koz-ATG*", Fig. 1a). Tandem DSBs introduced by the rare-cutting homing endonuclease, I-SceI, can release ("pop out") Koz-ATG, and religation of the DNA ends allows translation of *GFP* in the correct frame. We introduced, in parallel, two NHEJ reporters – one that generates fully cohesive 4 nucleotide (nt) overhangs (sGEJ) (Fig. 1b) and the other containing partially cohesive 4 nt overhangs (vGEJ; Fig. 1c) – into *Xrcc4*$^{flox/flox}$ mouse ES cells, where *Xrcc4* alleles can be conditionally deleted 33. We used Southern blotting to identify several clones that carry only one, intact, randomly integrated copy of the relevant NHEJ reporter. Background levels of GFP in each clone measured by fluorescence-activated cell sorting (FACS) were always < 0.01% (Supplementary Fig. 1). Expression of I-SceI, but not control empty vector, stimulated production of GFP in each cell type up to ∼40% in some reporter clones (Fig. 1b,c and Supplementary Fig 1). We used transient expression of the Cre recombinase to generate derivative clones of each reporter type that are either *Xrcc4*$^{+/+}$, *Xrcc4*$^{+/-}$ or *Xrcc4*$^{-/-}$ (confirmed by Southern analysis). Homozygous deletion of *Xrcc4* diminished the efficiency of NHEJ in all clones, but a robust residual end joining activity was noted in *Xrcc4*$^{-/-}$ cells (Fig. 1b,c). The emergence of GFP^{+} products of NHEJ was delayed in *Xrcc4*$^{-/-}$ cells compared to wild-type isogenic clones, implying that the kinetics of rejoining are slower in alternative NHEJ (Supplementary Fig. 2a,b). Expression of wild-type human *XRCC4* in *Xrcc4*$^{-/-}$ cells complemented the NHEJ defect (Supplementary Fig. 2c).

To determine whether components of the MRN complex influence NHEJ, we used siRNA to deplete Mre11 (siMre11) or Nbs1 (siNbs1) and measured the effect on I-SceI-induced NHEJ. Depletion of Mre11 reduced NHEJ in both *Xrcc4*$^{+/+}$ and *Xrcc4*$^{-/-}$ cells, whether the

reporter was sGEJ or vGEJ, in comparison to control luciferase siRNA (siLuc) (Fig. 1b,c). siNbs1 reduced NHEJ only in *Xrcc4*$^{+/+}$ cells, but Nbs1 depletion was incomplete; therefore a role for Nbs1 in *Xrcc4*-independent NHEJ, as observed recently in the context of V(D)J recombination, cannot be excluded (Fig. 1d) 31. Interestingly, the basal level of Mre11 was lower in *Xrcc4*$^{-/-}$ cells than in wild-type controls, the reasons for which are unclear. Despite this, robust knock-down of Mre11 by siMre11 was observed in each genetic background. Depletion of Mre11 or Nbs1 in HR reporter ES cells produced the expected reduction in I-SceI-induced HR (Supplementary Fig. 3a). The effects of Mre11 or Nbs1 depletion on NHEJ were also observed with use of a second set of independent siRNAs specific for Mre11 and Nbs1 (Supplementary Fig. 3b). Taken together, the data implicates Mre11 in both *Xrcc4*-dependent and *Xrcc4*-independent NHEJ, in mouse ES cells.

MRN activates the Atm signaling kinase at DSBs 3, and the effect of MRN deficiency on V(D)J recombination mimicks that of *Atm* deficiency 32. To determine whether Mre11 regulates NHEJ indirectly through Atm signaling, we examined NHEJ in the presence of the Atm inhibitor, KU55933. Despite evidence of Atm inhibition in KU55933-treated samples, no clear effect of KU55933 on NHEJ was observed in either *Xrcc4*$^{+/+}$ or *Xrcc4*$^{-/-}$ cells (Supplementary Fig. 4). Therefore, the NHEJ function of Mre11 does not require Atm signaling. However, a scaffolding function for Atm, or a qualitative contribution of Atm to NHEJ, as observed in V(D)J recombination 32, has not been excluded by our experiments.

To determine how Mre11 affects NHEJ qualitatively, we used FACS to clone individual I-SceI-induced GFP^{+} sGEJ reporter cells that had been co-transfected with either siMre11 or control siLuc, then expanded clones for preparation of genomic DNA (gDNA) and breakpoint sequencing. In *Xrcc4*$^{+/+}$ sGEJ reporter cells that had received control siLuc, 70% (49/70) of I-SceI-induced NHEJ were precise (Table 1 and Supplementary Fig. 5). Consistent with previous work, only 10.2% (5/49) of I-SceI-induced NHEJ events in isogenic *Xrcc4*$^{-/-}$ sGEJ reporter cells were precise 14. The remaining imprecise NHEJ events entailed deletions or, in a minority of cases, frame-shifts involving only the second I-SceI site (Table 1, Supplementary Fig. 5 and Supplementary Table 1). In *Xrcc4*$^{+/+}$ sGEJ reporter cells that received control siLuc, 76% (16/21) of imprecise NHEJ events entailed MMEJ. In isogenic *Xrcc4*$^{-/-}$ sGEJ reporter cells, 92% (35/38) of deletional repair events entailed MMEJ and 9% (6/64) of all imprecise rejoining events contained insertions at the breakpoint. Mre11 depletion did not affect the proportions of precise NHEJ in either *Xrcc4*$^{+/+}$ or *Xrcc4*$^{-/-}$ cells; however, Mre11 depletion reduced use of MMEJ in *Xrcc4*$^{+/+}$ sGEJ reporter cells, in comparison to control siLuc-treated cells (Table 1 and Supplementary Fig. 5). In siMre11-treated cells, 53% (9/17) of imprecise deletional NHEJ events entailed MMEJ, whereas the equivalent frequencies in control siLuc-treated cells was 76% (16/21; $P = 0.027$ by X^2 test). This effect is reminiscent of the known role of yeast *Mre11* in MMEJ 27.

To examine whether Mre11 influences processing of the DSB, we developed a new assay to quantify end processing in bulk cultures of sGEJ reporter cells undergoing I-SceI-induced NHEJ (Fig. 2). Near the tandem I-SceI sites are restriction sites for EcoRI, BglII and PstI. These sites are located to the left of the proximal I-SceI site at distances of 17 bp (EcoRI), 37 bp (BglII) and 64 bp (PstI) (Fig. 2a,b). If resection of the left I-SceI-induced DSB were

limited to less than 17 nt, the EcoRI site within the reporter would remain intact. In this case, gDNA restricted with NotI and EcoRI would generate a *GFP*-hybridizing band of 759 bp by Southern blotting. In contrast, in a clone that had undergone ≥ 17 nt resection of the left end of the DSB, the EcoRI site would be lost and gDNA restricted with NotI and EcoRI would reveal a larger *GFP*-hybridizing band of ∼3.2 kb by Southern blotting. This provides a way to quantify end processing during I-SceI-induced NHEJ (Fig. 2). We transfected *Xrcc4*$^{+/+}$ sGEJ reporter cells and isogenic *Xrcc4*$^{-/-}$ sGEJ reporter cells with an I-SceI plasmid and either siMre11, control siLuc or siRNA (siCtIP) to deplete the end processing protein, CtIP 21. We FACS sorted pools of I-SceI-induced GFP^{+} NHEJ products from each test group and prepared gDNA from these pools of cells. We digested gDNA from the different test groups with NotI alone or, in parallel, with NotI + I-SceI, NotI + EcoRI, NotI + BglII, or NotI + PstI, and analyzed restriction digested gDNA by Southern blotting, using a *GFP* probe (Fig. 2b).

As expected, deletion of *Xrcc4* generated more NHEJ products lacking the restriction sites close to the I-SceI site in the sGEJ reporter, as reflected by an increased intensity of the "uncut" ∼3.2 kb band in comparison to *Xrcc4*$^{+/+}$ test groups (Fig. 2b). In *Xrcc4*$^{-/-}$ cells, we noted a reduction in the intensity of this "uncut" band in siMre11-treated groups in comparison to those receiving either control siLuc or siCtIP (Fig. 2b). This suggests that Mre11 depletion reduces the probability that end processing will extend to the restriction sites close to the I-SceI site. We used phosphoimager and densitometry to quantify this effect, by measuring the relative intensity of ^{32}P-hybridizing bands for each treatment group. The probability that end processing had ablated a given restriction site was calculated as the ratio: ["Uncut":("Cut" + "Uncut") × 100]% (Fig. 2b,c and Supplementary Fig. 6). The results suggest that Mre11 promotes end processing during *Xrcc4*-independent NHEJ. In contrast, depletion of Mre11 in *Xrcc4*$^{+/+}$ cells did not diminish end processing in this assay. The reasons for this difference are not yet clear. However, MRN may have both scaffolding and enzymatic functions at the break, each of which might contribute to NHEJ 24,34,35.

Mammalian MRN binds the γ-H2A.X-interacting adaptor protein, Mdc1, during the *H2A.X*-dependent chromatin response to a DSB 4, and long-range end joining during class switch recombination (CSR) or fusion of dysfunctional telomeres is impaired in *H2A.X*$^{-/-}$ or *Mdc1*$^{-/-}$ cells 36-38. To determine whether the fraction of MRN that is associated with γ-H2A.X/Mdc1 contributes to NHEJ, we established an intact, single-copy NHEJ reporter sGEJ in *H2A.X*$^{flox/flox}$ mouse ES cells, where *H2A.X* alleles can be conditionally deleted 39, and used Cre treatment to generate isogenic *H2A.X*$^{-/-}$ sGEJ reporter clones. Homozygous deletion of *H2A.X*, whether or not accompanied by expression of wild-type *H2A.X* or the *S139A* mutant in *H2A.X*−/− sGEJ reporter cells, had no quantitative impact on NHEJ (Fig. 3a and Supplementary Fig. 7). Depletion of Mre11, Nbs1 or Brca1 reduced the efficiency of NHEJ in *H2A.X*$^{+/+}$ cells as efficiently as in isogenic *H2A.X*$^{-/-}$ cells (Fig. 3b), and we noted proportionate reductions in I-SceI-induced HR in *H2A.X*$^{+/+}$ and isogenic *H2A.X*$^{-/-}$ HR reporter cells (Fig. 3c). The basal level of Mre11 was slightly reduced in *H2A.X*$^{-/-}$ cells compared to wild-type cells, the reasons for which are unclear. However, depletion of Mre11 was equally efficient in these two isogenic ES cell lines (Fig. 3d). These results

suggest that the key NHEJ and HR functions of Mre11, Nbs1 and Brca1 are executed independently of *H2A.X*.

DISCUSSION

Using a single-copy, chromosomally integrated NHEJ reporter, in which NHEJ can be triggered by a site-specific DSB, we show that Mre11 is required for efficient *Xrcc4*-dependent and *Xrcc4*-independent NHEJ in mouse ES cells. Southern analysis of NHEJ in *Xrcc4*$^{-/-}$ cells reveals that Mre11 depletion reduces the extent of deletions associated with error-prone NHEJ. This suggests that endogenous Mre11 normally contributes to processing of the DSB during *Xrcc4*-independent NHEJ. We find that both the NHEJ and HR functions of Mre11 and Nbs1 are independent of *H2AX*.

MRN is one of many DSB response protein complexes that accumulate on chromatin marked by γ-H2AX (the "chromatin domain" of the DSB response – Fig. 4). γ-H2AX and its adaptor protein, Mdc1, have defined functions in DSB repair during sister chromatid recombination and CSR 37,40-43. Interestingly, although the association of MRN, 53bp1 and Brca1 with the "chromatin domain" of the DSB response is dependent on *H2A.X*, these proteins can also accumulate in the "DNA domain" of the DSB response (Fig. 4) in cells lacking *H2A.X* or *Mdc1* 5,44. Importantly, the DSB repair functions of MRN, 53bp1 and Brca1 are in part independent of *H2A.X* (Fig. 3) 37,42,43, suggesting that MRN, 53bp1 and Brca1 execute their DSB repair functions primarily in association with the "DNA domain" of the DSB response.

The roles of *Mre11* in DSB repair have been studied extensively in lower eukaryotes. *S. cerevisiae mre11* null mutants reveal inefficient religation of both cohesive and mismatched ends, and this is reversed by expression of either wild-type or nuclease-defective *mre11* alleles 25,45,46. This suggests that one function of Mre11 in NHEJ is as a scaffold to support synapsis 46-48. In contrast, *mre11* nuclease-defective mutants reveal a defect in MMEJ, suggesting that the Mre11 nuclease resects DNA ends and exposes tracts of microhomology 46,49. In the experiments reported here, Mre11 depletion in *Xrcc4*$^{+/+}$ mammalian cells reduced the efficiency of NHEJ but did not affect the strong preference for precise end joining. Since precise NHEJ does not entail end resection, the role of Mre11 in this pathway may be to support synapsis between the two DNA ends, thereby promoting religation of the DSB (Fig. 4). A recent structural analysis of *Pyrococcus furiosus* Mre11 is consistent with such a role for Mre11 24. In contrast, in *Xrcc4*$^{-/-}$ cells, Mre11 appears to have additional functions in DSB processing, leading to the generation of extensive deletions during error-prone NHEJ or MMEJ (Fig. 4). Definitive evidence of the relative contributions of Mre11 scaffolding and nuclease functions to mammalian NHEJ will require complementation experiments in cells lacking *Mre11*.

Mammalian NHEJ factors repair unscheduled chromosomal DSBs and also mediate the fusion of dysfunctional telomeres and specialized recombination reactions in the immune system, such as V(D)J recombination and CSR 11,12,50. It is not yet clear to what extent the "rules" governing one NHEJ process apply to other contexts. Our results illustrate a difference between short-range NHEJ (studied here), which is *H2A.X*-independent, and

long-range NHEJ processes that are partially *H2A.X*-dependent 36-38. It will be interesting to determine how the distance between the two DSBs influences the quality of DSB repair and its genetic dependencies. Similarly, the regulation of NHEJ has been shown to vary according to cell type 51,52, raising the possibility that our findings are restricted to mouse ES cells. However, recent work implicates MRN in NHEJ in several different cell types, suggesting a general role in NHEJ31,32 **[+ 53, 54 Ferguson, Lopez papers in press, NSMB]**. In addition to the effects on DNA damage signaling and HR, *Mre11* dysfunction may promote genomic instability and cancer in mammals by disabling NHEJ.

ONLINE METHODS

Plasmid and siRNA

To construct the NHEJ reporter sGEJ, we purchased from Invitrogen the 70-mer oligo containing two sequential I-SceI sites and the artificial Kozak-ATG translation sequence (5′-cggaattcattaccctgttatccctaaccgccgccaccatggattaccctgttatccctacggatcc-3′) and its complementary 70-mer, annealed, digested with EcoRI and BamHI and inserted into the EcoRI-BamHI site of pcDNA3-EGFP-SnaBI where a silence mutation was introduced into the *GFP* gene by PCR to generate an SnaBI site (5′-tacgta-3′) using oligo 5′-ccaccctcgtgaccacccttacgtacggc-3′. We replaced the original *GFP* translation site (5′-gccaccatggtg-3′) with 5′-cttcacatgatc-3′ by PCR using primers 5′-tgggatccatccttcacatgatcagcaagggcgaggagctgttc-3′ and 5′-gccgtacgtaagggtggtcacgagggtgg-3′ to generate pcDNA3-sGEJ. We generated the final ROSA26-PA NHEJ targeting vector sGEJ using an approach described previously 42. We similarly constructed the NHEJ reporter vGEJ containing two inverted I-SceI sites. The hygromycin resistant (Hyg^R) expression vectors for *Xrcc4* and HA-tagged wild-type *H2A.X* and its *S139A* mutant were constructed as described previously 42,43. We purchased RNAi duplex targeting *luciferase* control (cgtacgcggaatacttcga), mouse *Mre11* (#1: gctgcttggagctgcttag; #2: acaggagaagagatcaact), *Nbs1* (#1: gacaggagatagagttacc; #2: gcagttgaatctaagaaac), *Brca1* (ccagaagaaagggccttca) and *CtIP* (ggaactctggacaaaacta) from Dharmacon.

Cell lines and cell culture

We grew $Xrcc4^{flox/flox}$ and $H2A.X^{flox/flox}$ mouse ES cells 33,39 in ES medium on either mouse embryonic fibroblast (MEF) feeder cells or gelatinized plates. We established $Xrcc4^{flox/flox}$ and $H2A.X^{flox/flox}$ NHEJ reporter ES clones harboring a single, intact, randomly integrated copy of the NHEJ reporter as described previously for the establishment of the HR reporter mouse ES cells 42,43. We generated isogenic $Xrcc4^{+/+}$ and $Xrcc4^{-/-}$ and isogenic $H2A.X^{+/+}$ and $H2A.X^{-/-}$ ES reporter clones using adeno-Cre infection as described previously 42,43. To generate $Xrcc4^{-/-}$ ES cells stably expressing wild-type human *XRCC4*, we electroporated 6×10^6 $Xrcc4^{-/-}$ ES cells with 8 mg of Hyg^R *XRCC4* expression vector and seeded them on a 10 cm plate. We added hygromycin (400 μg ml^{-1}) 48 hr later to select Hyg^R clones which were expanded ∼7 days later.

Antibodies and Western blotting

Commercial antibodies used in this study were mouse monoclonal anti-β-actin (Cat# ab8226) and rabbit polyclonal anti-Mre11 (Cat# ab397) from Abcam, rabbit polyclonal anti-

Nbs1 (Cat# NB100-60648) from Novus Biologicals, rabbit polyclonal anti-HA-tag (Cat# sc-805) and anti-p53 (Cat# sc-6243) and goat polyclonal anti-human XRCC4 (Cat# sc-8285) from Santa Cruz Biotechnology, rabbit polyclonal anti-histone H4 (Cat# 06-598) from Upstate, and rabbit polyclonal anti-phospho-p53 Ser15 (Cat# 9284) from Cell Signaling. Rabbit polyclonal anti-mouse Brca1 antibody was from Junjie Chen. We analyzed histones and non-histone proteins by Western blotting as described before 42.

Sequence analysis and Southern blotting

To sequence repair junctions of I-SceI-induced NHEJ products, we sorted individual I-SceI-induced GFP^+ cells using a 4-laser BD FACSAria (BD Biosciences) and expanded them as clones. We prepared gDNA from expanded GFP^+ clones as described previously 42. We amplified sequences containing the repair junctions by PCR using primers #1 (tgcacgcttcaaaagcgcacg) and #2 (ctcctggacgtagccttcgggg). We purified PCR products and had them sequenced using nested primers #3 (ccgcgctgttctcctcttc) and #4 (gccgtacgtaagggtggtcacgagggtgg). For Southern blotting, we FACS sorted I-SceI-induced GFP^+ cells as pools and expanded. We purified gDNA from the sorted, expanded pools of GFP^+ cells, digested with relevant restriction enzymes and analyzed by Southern blotting using the *GFP* cDNA as a probe 42.

I-SceI-induced repair assays

To analyze I-SceI-induced GFP^+ frequencies in NHEJ or HR reporter mouse ES cells, we transfected I-SceI expression plasmids into these reporter cells as described previously 42,43 to induce a break and thus NHEJ or HR42,43. We performed parallel transfection of a wild-type *GFP* expression vector, at an amount one tenth of that of the I-SceI expression vector, to determine transfection efficiency. Unless otherwise stated, statistical analysis was by Student's two-tailed unpaired *t*-test (unknown variance) or, for paired samples, by Student's two-tailed paired *t*-test.

Atm inhibition

We prepared Atm kinase inhibitor KU55933 (Calbiochem, Cat# 118500) and DNA-PKcs inhibitor NU7026 (Sigma, Cat# N1537) in DSMO as 10 mM stock solutions and diluted to a final concentration of 20 μM for KU55933 and 40 μM for NU7026 for I-SceI-induced repaired assays. In these assays, we added these inhibitors at 22 hrs post-transfection. After incubation for additional 72 hrs, we analyzed cells for NHEJ levels using flow cytometry. For effect of Atm inhibition on ionizing radiation (IR)-induced phosphorylation of p53 Ser15 and H2A.X Ser139, we preincubated cells in media with chemical inhibitors for 1 hr, exposed to 5 Gy of irradiation, incubated for another 2 hrs and lysed for Western blotting.

Supplementary Material

Refer to Web version on PubMed Central for supplementary material.

ACKNOWLEDGEMENTS

We thank Dr. Frederick Alt, Dr. Catherine Yan and members of the Scully lab for helpful discussions, and Drs. Bernard Lopez, David Ferguson and Sandy Chang for discussions and for sharing data prior to publication. This

work was supported by R01s CA095175 and GM073894 and a Leukemia and Lymphoma Society Scholar Award (to R.S.).

REFERENCES

1. Williams RS, Williams JS, Tainer JA. Mre11-Rad50-Nbs1 is a keystone complex connecting DNA repair machinery, double-strand break signaling, and the chromatin template. Biochem Cell Biol. 2007; 85:509–20. [PubMed: 17713585]
2. Berkovich E, Monnat RJ Jr. Kastan MB. Roles of ATM and NBS1 in chromatin structure modulation and DNA double-strand break repair. Nat Cell Biol. 2007; 9:683–90. [PubMed: 17486112]
3. Lee JH, Paull TT. ATM activation by DNA double-strand breaks through the Mre11-Rad50-Nbs1 complex. Science. 2005; 308:551–4. [PubMed: 15790808]
4. Stucki M, Jackson SP. gammaH2AX and MDC1: anchoring the DNA-damage-response machinery to broken chromosomes. DNA Repair (Amst). 2006; 5:534–43. [PubMed: 16531125]
5. Bekker-Jensen S, et al. Spatial organization of the mammalian genome surveillance machinery in response to DNA strand breaks. J Cell Biol. 2006; 173:195–206. [PubMed: 16618811]
6. Luo G, et al. Disruption of mRad50 causes embryonic stem cell lethality, abnormal embryonic development, and sensitivity to ionizing radiation. Proc Natl Acad Sci U S A. 1999; 96:7376–81. [PubMed: 10377422]
7. Xiao Y, Weaver DT. Conditional gene targeted deletion by Cre recombinase demonstrates the requirement for the double-strand break repair Mre11 protein in murine embryonic stem cells. Nucleic Acids Research. 1997; 25:2985–91. [PubMed: 9224597]
8. Zhu J, Petersen S, Tessarollo L, Nussenzweig A. Targeted disruption of the Nijmegen breakage syndrome gene NBS1 leads to early embryonic lethality in mice. Curr Biol. 2001; 11:105–9. [PubMed: 11231126]
9. Stewart GS, et al. The DNA double-strand break repair gene hMRE11 is mutated in individuals with an ataxia-telangiectasia-like disorder. Cell. 1999; 99:577–87. [PubMed: 10612394]
10. Carney JP, et al. The hMre11/hRad50 protein complex and Nijmegen breakage syndrome: linkage of double-strand break repair to the cellular DNA damage response. Cell. 1998; 93:477–86. [PubMed: 9590181]
11. Dudley DD, Chaudhuri J, Bassing CH, Alt FW. Mechanism and control of V(D)J recombination versus class switch recombination: similarities and differences. Adv Immunol. 2005; 86:43–112. [PubMed: 15705419]
12. Lieber MR. The mechanism of human nonhomologous DNA end joining. J Biol Chem. 2008; 283:1–5. [PubMed: 17999957]
13. Corneo B, et al. Rag mutations reveal robust alternative end joining. Nature. 2007; 449:483–6. [PubMed: 17898768]
14. Guirouilh-Barbat J, Rass E, Plo I, Bertrand P, Lopez BS. Defects in XRCC4 and KU80 differentially affect the joining of distal nonhomologous ends. Proc Natl Acad Sci U S A. 2007; 104:20902–7. [PubMed: 18093953]
15. Soulas-Sprauel P, et al. Role for DNA repair factor XRCC4 in immunoglobulin class switch recombination. J Exp Med. 2007; 204:1717–27. [PubMed: 17606631]
16. Yan CT, et al. IgH class switching and translocations use a robust non-classical end-joining pathway. Nature. 2007; 449:478–82. [PubMed: 17713479]
17. Haber JE. Alternative endings. Proc Natl Acad Sci U S A. 2008; 105:405–6. [PubMed: 18180452]
18. Limbo O, et al. Ctp1 is a cell-cycle-regulated protein that functions with Mre11 complex to control double-strand break repair by homologous recombination. Mol Cell. 2007; 28:134–46. [PubMed: 17936710]
19. Mimitou EP, Symington LS. Sae2, Exo1 and Sgs1 collaborate in DNA double-strand break processing. Nature. 2008; 455:770–4. [PubMed: 18806779]
20. Zhu Z, Chung WH, Shim EY, Lee SE, Ira G. Sgs1 helicase and two nucleases Dna2 and Exo1 resect DNA double-strand break ends. Cell. 2008; 134:981–94. [PubMed: 18805091]

21. Sartori AA, et al. Human CtIP promotes DNA end resection. Nature. 2007; 450:509–14. [PubMed: 17965729]
22. Bhaskara V, et al. Rad50 adenylate kinase activity regulates DNA tethering by Mre11/Rad50 complexes. Mol Cell. 2007; 25:647–61. [PubMed: 17349953]
23. Stracker TH, Theunissen JW, Morales M, Petrini JH. The Mre11 complex and the metabolism of chromosome breaks: the importance of communicating and holding things together. DNA Repair (Amst). 2004; 3:845–54. [PubMed: 15279769]
24. Williams RS, et al. Mre11 dimers coordinate DNA end bridging and nuclease processing in double-strand-break repair. Cell. 2008; 135:97–109. [PubMed: 18854158]
25. Moore JK, Haber JE. Cell cycle and genetic requirements of two pathways of nonhomologous end-joining repair of double-strand breaks in Saccharomyces cerevisiae. Mol Cell Biol. 1996; 16:2164–73. [PubMed: 8628283]
26. Chen L, Trujillo K, Ramos W, Sung P, Tomkinson AE. Promotion of Dnl4-catalyzed DNA end-joining by the Rad50/Mre11/Xrs2 and Hdf1/Hdf2 complexes. Molecular Cell. 2001; 8:1105–15. [PubMed: 11741545]
27. Ma JL, Kim EM, Haber JE, Lee SE. Yeast Mre11 and Rad1 proteins define a Ku-independent mechanism to repair double-strand breaks lacking overlapping end sequences. Mol Cell Biol. 2003; 23:8820–8. [PubMed: 14612421]
28. Huang J, Dynan WS. Reconstitution of the mammalian DNA double-strand break end-joining reaction reveals a requirement for an Mre11/Rad50/NBS1-containing fraction. Nucleic Acids Research. 2002; 30:667–74. [PubMed: 11809878]
29. Zhong Q, Boyer TG, Chen PL, Lee WH. Deficient nonhomologous end-joining activity in cell-free extracts from Brca1-null fibroblasts. Cancer Research. 2002; 62:3966–70. [PubMed: 12124328]
30. Di Virgilio M, Gautier J. Repair of double-strand breaks by nonhomologous end joining in the absence of Mre11. J Cell Biol. 2005; 171:765–71. [PubMed: 16330708]
31. Deriano L, Stracker TH, Baker A, Petrini JH, Roth DB. Roles for NBS1 in alternative nonhomologous end-joining of V(D)J recombination intermediates. Mol Cell. 2009; 34:13–25. [PubMed: 19362533]
32. Helmink BA, et al. MRN complex function in the repair of chromosomal Rag-mediated DNA double-strand breaks. J Exp Med. 2009; 206:669–79. [PubMed: 19221393]
33. Yan CT, et al. XRCC4 suppresses medulloblastomas with recurrent translocations in p53-deficient mice. Proc Natl Acad Sci U S A. 2006; 103:7378–83. [PubMed: 16670198]
34. de Jager M, et al. Human Rad50/Mre11 is a flexible complex that can tether DNA ends. Mol Cell. 2001; 8:1129–35. [PubMed: 11741547]
35. Hopfner KP, et al. The Rad50 zinc-hook is a structure joining Mre11 complexes in DNA recombination and repair. Nature. 2002; 418:562–6. [PubMed: 12152085]
36. Reina-San-Martin B, et al. H2AX is required for recombination between immunoglobulin switch regions but not for intra-switch region recombination or somatic hypermutation. J Exp Med. 2003; 197:1767–78. [PubMed: 12810694]
37. Franco S, et al. H2AX prevents DNA breaks from progressing to chromosome breaks and translocations. Mol Cell. 2006; 21:201–14. [PubMed: 16427010]
38. Dimitrova N, de Lange T. MDC1 accelerates nonhomologous end-joining of dysfunctional telomeres. Genes Dev. 2006; 20:3238–43. [PubMed: 17158742]
39. Bassing CH, et al. Increased ionizing radiation sensitivity and genomic instability in the absence of histone H2AX. Proc Natl Acad Sci U S A. 2002; 99:8173–8. [PubMed: 12034884]
40. Celeste A, et al. Genomic instability in mice lacking histone H2AX. Science. 2002; 296:922–7. [PubMed: 11934988]
41. Lou Z, et al. MDC1 maintains genomic stability by participating in the amplification of ATM-dependent DNA damage signals. Mol Cell. 2006; 21:187–200. [PubMed: 16427009]
42. Xie A, et al. Control of sister chromatid recombination by histone H2AX. Mol Cell. 2004; 16:1017–25. [PubMed: 15610743]
43. Xie A, et al. Distinct roles of chromatin-associated proteins MDC1 and 53BP1 in mammalian double-strand break repair. Mol Cell. 2007; 28:1045–57. [PubMed: 18158901]

44. Celeste A, et al. Histone H2AX phosphorylation is dispensable for the initial recognition of DNA breaks. Nat Cell Biol. 2003; 5:675–9. [PubMed: 12792649]
45. Boulton SJ, Jackson SP. Components of the Ku-dependent non-homologous end-joining pathway are involved in telomeric length maintenance and telomeric silencing. Embo J. 1998; 17:1819–28. [PubMed: 9501103]
46. Zhang X, Paull TT. The Mre11/Rad50/Xrs2 complex and non-homologous end-joining of incompatible ends in S. cerevisiae. DNA Repair (Amst). 2005; 4:1281–94. [PubMed: 16043424]
47. Lee SE, Bressan DA, Petrini JH, Haber JE. Complementation between N-terminal Saccharomyces cerevisiae mre11 alleles in DNA repair and telomere length maintenance. DNA Repair (Amst). 2002; 1:27–40. [PubMed: 12509295]
48. Moreau S, Morgan EA, Symington LS. Overlapping functions of the Saccharomyces cerevisiae Mre11, Exo1 and Rad27 nucleases in DNA metabolism. Genetics. 2001; 159:1423–33. [PubMed: 11779786]
49. Zhang Y, et al. Role of Dnl4-Lif1 in nonhomologous end-joining repair complex assembly and suppression of homologous recombination. Nat Struct Mol Biol. 2007; 14:639–46. [PubMed: 17589524]
50. Riha K, Heacock ML, Shippen DE. The role of the nonhomologous end-joining DNA double-strand break repair pathway in telomere biology. Annu Rev Genet. 2006; 40:237–77. [PubMed: 16822175]
51. Gao Y, et al. A targeted DNA-PKcs-null mutation reveals DNA-PK-independent functions for KU in V(D)J recombination. Immunity. 1998; 9:367–76. [PubMed: 9768756]
52. Li G, et al. Lymphocyte-specific compensation for XLF/cernunnos end-joining functions in V(D)J recombination. Mol Cell. 2008; 31:631–40. [PubMed: 18775323]
53. Ferguson paper on Mre11, in press, NSMB.
54. Lopez paper on Mre11, in press, NSMB.

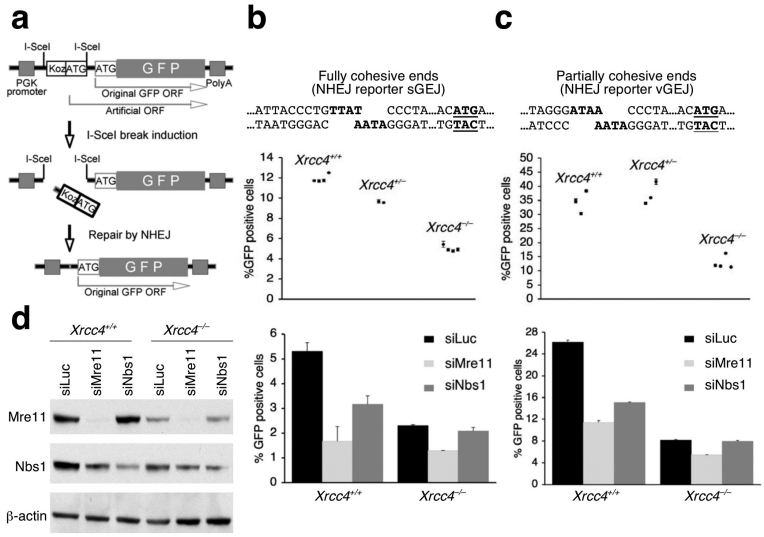

Figure 1.

Mre11 regulates both *Xrcc4*-dependent and *Xrcc4*-independent NHEJ. (**a**) Structure of the NHEJ reporter. PGK: *phosphoglycerate kinase*. "Koz-ATG": an artificial Kozak-ATG translation start site. ORF: open reading frame. PolyA: polyadenylation signal. (**b, c**) I-SceI-induced NHEJ in $Xrcc4^{+/+}$ and $Xrcc4^{-/-}$ isogenic mouse ES cells containing the sGEJ reporter (**b**) or the vGEJ reporter (**c**). In upper sections, each point represents the mean of triplicates in one experiment for each reporter clone; error bars indicate standard error of mean (s.e.m). Unpaired *t*-test (unknown variance) for $Xrcc4^{-/-}$ cells *versus* $Xrcc4^{+/+}$ cells, $P = 0.00000037$ (**b**) or $P = 0.0038$ (**c**); for $Xrcc4^{-/-}$ cells *versus* $Xrcc4^{+/-}$ cells, $P = 0.000015$ (**b**) or $P = 0.0025$ (**c**). In lower sections, $Xrcc4^{+/+}$ and $Xrcc4^{-/-}$ NHEJ reporter cells were co-transfected with siRNA to Mre11 (siMre11), Nbs1 (siNbs1), or control luciferase (siLuc), together with I-SceI expression plasmids. Percentages of I-SceI-induced GFP^+ cells were measured. Bars represent the mean of triplicates in one representative experiment. Error bars indicate s.e.m. Student's paired *t*-test (two-tailed): in $Xrcc4^{+/+}$ cells, siMre11 *versus* siLuc, $P = 0.00045$ (**b**) and $P = 0.000035$ (**c**); siNbs1 *versus* siLuc, $P = 0.0037$ (**b**) and $P = 0.0012$ (**c**); in $Xrcc4^{-/-}$ cells, siMre11 *versus* siLuc, $P = 0.0037$ (**b**) and $P = 0.0018$ (**c**); siNbs1 *versus* siLuc, $P = 0.07$ (**b**) and $P = 0.467$ (**c**). (**d**) Protein abundance in $Xrcc4^{+/+}$ and $Xrcc4^{-/-}$ NHEJ reporter mouse ES cells treated with siRNAs shown. Whole cell extracts were analyzed three days after siRNA transfection. β-actin is a loading control.

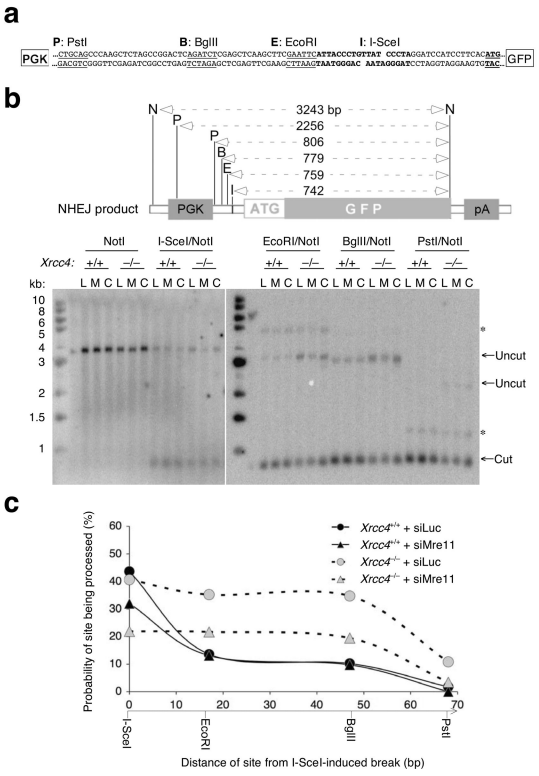

Figure 2.

Mre11 promotes end processing in *Xrcc4*-independent NHEJ.**(a)** Junction sequence of the NHEJ reporter sGEJ "pop-out" product (i.e., with excision of the Kozak-ATG translation start site). Sequences of two partial I-SceI sites are indicated in bold. Start codon of the *GFP* ORF is in bold and underlined. Restriction sites in the reporter are as follows. P: PstI; B: BglII; E: EcoRI; I: I-SceI. PGK: *phopshoglycerate kinase* promoter. (**b**) Structural analysis of pooled I-SceI-induced GFP^{+} NHEJ products. Upper section shows sizes of expected *GFP*-hybridizing restriction fragment sizes following digestion of gDNA with enzymes shown (I: I-SceI; E: EcoRI; B: BglII; P; PstI; N: NotI). Lower section shows Southern blot analysis of gDNA from pooled I-SceI-induced GFP^{+} NHEJ products from *Xrcc4*$^{+/+}$ and *Xrcc4*$^{-/-}$ sGEJ reporter mouse ES cells co-transfected with I-SceI expression vector and either control siLuc (L) or test siMre11 (M) or siCtIP (siRNA to CtIP) (C). Southern blots were probed with *GFP* cDNA. Arrows indicate NHEJ products that had either retained ("Cut") or lost ("Uncut") the relevant I-SceI-proximal restriction site. PGK: *phopshoglycerate kinase* promoter. pA: polyadenylation signal. *: non-specific hybridization product. (**c**) Effect of *Xrcc4* status and Mre11 depletion on the probability of restriction sites being processed during NHEJ, calculated from the intensities of the DNA bands in the Southern blot in (**b**), quantified by phosphoimager and densitometry, as the intensity of the "uncut" band divided by the combined intensities of "cut" and "uncut" bands (expressed as a percentage). The probability is plotted against the distance of each site from the I-SceI-induced break indicated along the *x*-axis.

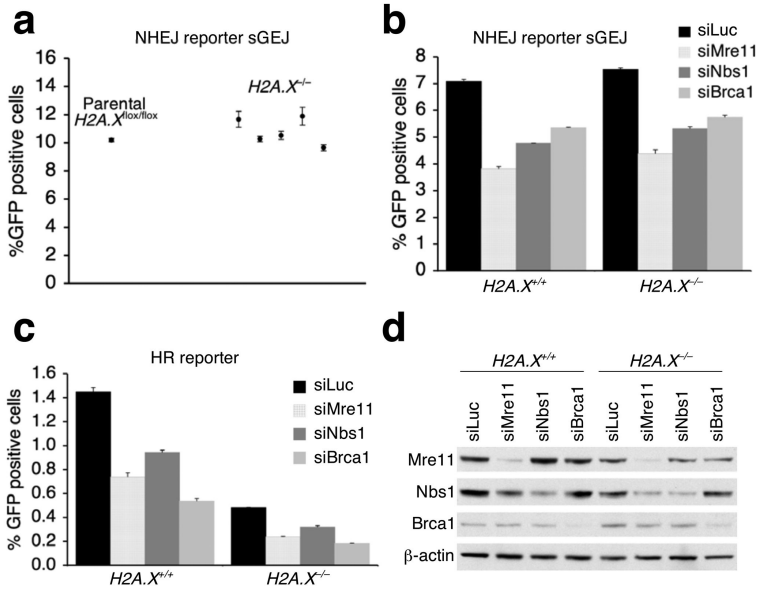

Figure 3.

The HR and NHEJ function of Mre11 is at least in part independent of *H2A.X*. (**a**) I-SceI-induced NHEJ in parental $H2A.X^{+/+}$ and isogenic $H2A.X^{-/-}$ sGEJ NHEJ reporter mouse ES clones. Points represent mean of triplicates for independent clones. Error bars indicate s.e.m. (**b**, **c**) Percentage of I-SceI-induced GFP^{+} cells from $H2A.X^{+/+}$ and $H2A.X^{-/-}$ sGEJ reporter mouse ES cells (**b**) or HR reporter mouse ES cells (**c**) depleted of Mre11, Nbs1 or Brca1 by siRNA duplex, with siLuc as a control. Bars represent mean of triplicates. Error bars indicate s.e.m. Student's paired *t*-test (two-tailed) in (**b**): in $H2A.X^{+/+}$ cells, siLuc versus siMre11, $P = 0.000048$; versus siNbs1, $P = 0.0009$; versus siBrca1, $P = 0.0024$; in $H2A.X^{-/-}$ cells, siLuc versus siMre11, $P = 0.00089$; versus siNbs1, $P = 0.0013$; versus siBrca1, $P = 0.0046$. Student's paired *t*-test in (**c**): in $H2A.X^{+/+}$ cells, siLuc versus siMre11, $P = 0.0023$; versus siNbs1, $P = 0.0046$; versus siBrca1, $P = 0.00026$; in $H2A.X^{-/-}$ cells, siLuc versus siMre11, $P = 0.00055$; versus siNbs1, $P = 0.0059$; versus siBrca1, $P = 0.000043$. (**d**) Steady state protein levels in $H2A.X^{+/+}$ and $H2A.X^{-/-}$ reporter mouse ES cells treated with indicated siRNAs. Whole cell extracts were analyzed by Western blotting three days after siRNA transfection. β-actin serves as a loading control.

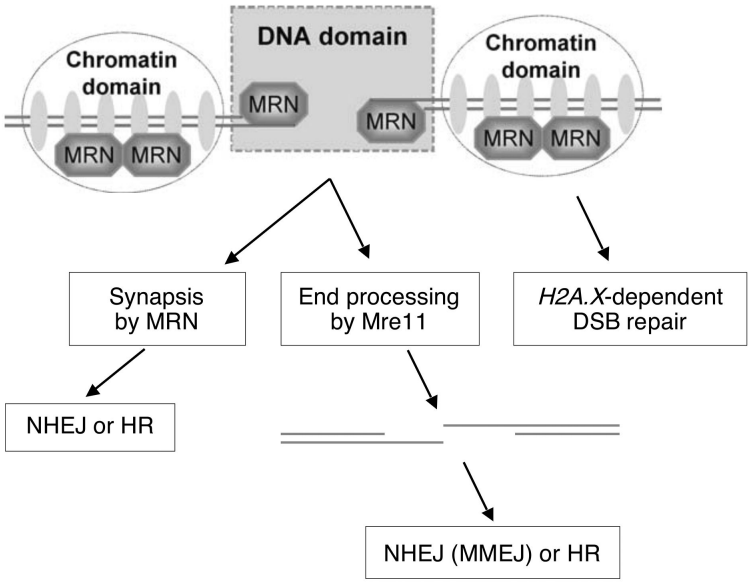

Figure 4.

Model for MRN's functions at a mammalian DSB. Mre11 nuclease activity may resect the DNA ends for either HR or *Xrcc4*-independent NHEJ/MMEJ. MRN may also promote synapsis during NHEJ (and possibly during HR). “Short-range” NHEJ of repairable DSBs by MRN appears to be independent of *H2A.X*.

Table 1

I-SceI-induced NHEJ products in sGEJ reporter cells

	Number of repair events				Percentage of all NHEJ events (%)			
	Xrcc4 $^{+/+}$		*Xrcc4* $^{-/-}$		*Xrcc4* $^{+/+}$		*Xrcc4* $^{-/-}$	
	siLuc	**siMre11**	**siLuc**	**siMre11**	**siLuc**	**siMre11**	**siLuc**	**siMre11**
Accurate repair	49	48	5	8	70	72.7	10.2	12.5
Deletions								
+ microhomologies	16	9	35	44	22.9	13.6	71.4	68.8
no microhomologies	5	8	3	6	7.1	12.1	6.1	9.4
Deletions+insertions	-	1	3	3	-	1.5	6.1	4.7
Insertions	-	-	3	3	-	-	6.1	4.7
Total repair events	70	66	49	64	100.0	100.0	100.0	100.0

Nat Struct Mol Biol. Author manuscript; available in PMC 2010 February 01.